DOI: 10.21062/mft.2023.037 http://www.journalmt.com

Advances in Surface Laser Cladding Remanufacturing of Shaft Parts

Changlong Zhao (0000-0001-7778-3494), Junbao Yang (0000-0002-4958-6546), Ming Li (0000-0003-4202-0256), Qinxiang Zhao (0000-0002-6584-0196), Hongnan Ma (0000-0003-2906-2486), Xiaoyu Jia (0000-0003-4843-9947), Haifeng Zhang*
[1]College of mechanical and vehicle engineering, Changchun University, Changchun, Jilin Province, China. E-mail: zhao19790204@126.com; 2547025748@qq.com.

This paper provides an overview of the commonly used processes and equipment for laser cladding, including pre-set powder feeding, simultaneous powder feeding, wire feeding cladding, and coaxial cladding nozzles. By comparing the above processes and related nozzles, the coating characteristics are summarized for the selection of appropriate methods and equipment in different working environments. Meanwhile, the morphology and properties of the clad layers of shaft parts processed with different process parameters (e.g. laser power, scanning speed, lap rate, powder feed rate) and the influence of the combined parameters are overviewed. The changes and mechanisms of metals, ceramics, and metal-ceramic composites in terms of hardness, wear resistance, metallurgical bonding, and microstructure are analyzed. In addition, the application of numerical simulation techniques to simulate the temperature and stress fields and to plan the melting trajectory when laser cladding processing is performed on the surface of shaft parts are reviewed. Finally, the problems in the current research on laser cladding of shaft parts are summarized and the development directions are discussed.

Keywords: Shaft part, Laser cladding, Process parameters, Cladding materials

1 Introduction

Shaft parts such as optical shafts, stepped shafts, solid shafts, shaped shafts, etc. in the system to support the transmission parts, bearing the load and the role of torque transmission, are the key foundation parts in mechanical equipment. However, shaft parts in long-term service are prone to wear, burns, abrasions, and fatigue fractures, which can affect working accuracy or even fail, and pose a serious threat to machine and personal safety if not treated in time[1]. Laser cladding has the advantages of concentrated heat, small heat-affected zone, fast melting, fast cooling, and less deformation. The higher the temperature gradient, the better the directional solidification growth of the material, resulting in coatings with enhanced material properties such as metallurgical properties, corrosion resistance, high hardness, and corrosion resistance. This feature can be used to repair and strengthen metal surfaces, thereby increasing the life of the product. Researchers are working to obtain better coating performance to expand the use of laser cladding processes on shaft components. This paper focuses on an overview of the characteristics of the laser cladding process and equipment, the influence of the process parameters and the choice of cladding material on the coating dilution, hardness, and surface morphology, as well as numerical simulations as an auxiliary application in the experiments, and finally prospects for the application of laser cladding remanufacturing technology on shaft parts.

2 Laser cladding processes and equipment

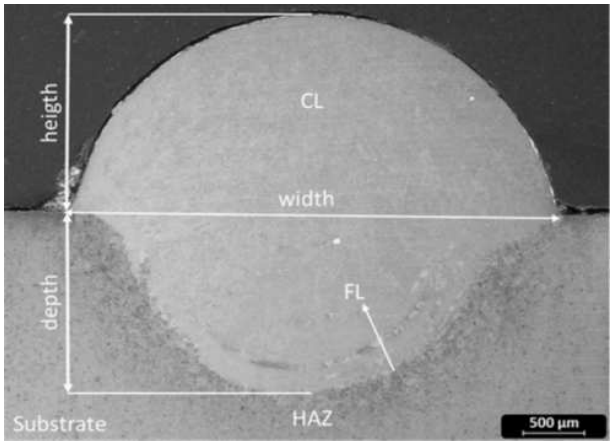

Fig. 1 *Laser clad specimen*

Shaft components suffer from random alternating loads for a long time and are prone to wear and even fracture failure under severe working conditions. High-strength, wear-resistant alloy cladding layers are prepared on shaft surfaces using laser cladding technology, which is intended to allow surface modification, repair, or additive manufacturing. The processed clad specimen usually consists of four parts (as in Figure 1): clad layer zone (CL), fusion line (FL), heat affected zone (HAZ), and substrate (SUB), which

is a complex process covering aspects of physics, chemistry and metallurgy.Choosing the right process method and equipment is beneficial to improving the cladding efficiency and obtaining good cladding layer properties.

2.1 Process methods

The laser cladding process is divided into three categories according to the different feeding methods and material forms of the cladding material: pre-set powder feeding, synchronous powder feeding, and wire feeding cladding. Pre-set powder feeding is to pre-set the coating powder on the substrate, and the pre-set powder is melted and solidified together with the substrate to obtain the coating layer, as shown in Figure 2(a). Synchronous powder feeding is to feed the molten powder directly into the beam and form the molten layer as the beam moves over the workpiece surface. There are two ways to achieve synchronous powder feeding, one is coaxial powder feeding, as shown in Figure 2(b). The other is off-axis powder feeding, as shown in Figure 2(c). Wire feeding cladding is to feed a metal wire into the beam to melt and solidify with the substrate to achieve the laser cladding layer[2], as shown in Figure 2(d).

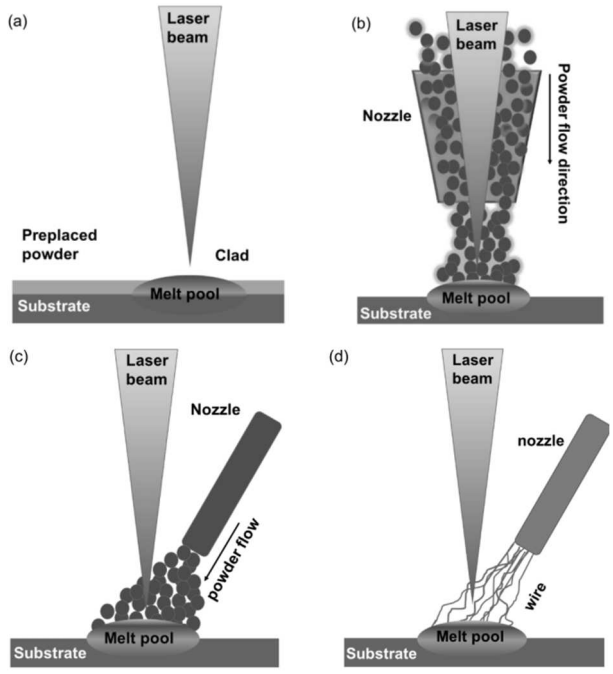

Fig. 2 *Conceptual diagram of pre-set powder (a), off-axis powder feeding (b), coaxial powder feeding (c), wire feeding cladding system (d)*

Experimental studies have been carried out to understand the changes in the quality state of the clad layer under each process to select the appropriate cladding method for the experiments. Abioye T E. et al.[3] used similar processing parameters to clad 625 alloy powder and wire respectively on the surface of the AISI 304 substrate. Both formed good metallurgical structures with no obvious defects inside the molten layer. The wire feeding system showed better performance quality and dimensional accuracy during continuous single-track laser cladding processing. It was demonstrated that the molten layer using powder specimens had higher dilution, finer dendritic microstructure, higher density of dendritic precipitates, and showed higher hardness.

Farayibi, P. K. et al.[4] used a co-feed of powder and wire to fuse Ti-6Al-4V wire and WC/W2C powder onto the Ti-6Al-4V substrate surface using the Taguchi technique and regression model. The signal-to-noise ratio of the melted layer was 36.67 and the geometric aspect ratio was 0.4, which is within a reasonable range. The experiments showed that raising the laser power significantly increased the cladding layer width and lowering the scanning speed increased the cladding layer height.

A three-dimensional numerical model to study the powder flow structure of coaxially fed powder was developed by Liu H et al.[5] And their predicted powder flow structure agreed well with the experimental results. It was found that the factors affecting the velocity vector and convergence characteristics at the nozzle exit are the particle diameter of the melt material and the recovery coefficient. The convergence characteristics are specifically generated by the collisions between the powder streams below the nozzle. It was concluded that if the diameter of the particles is not greater than 100 μm, the number of collisions is higher at 14 and the velocity at the tip of the nozzle is lower at about 0.4 m/s. Conversely, if the particle diameter exceeds 100 microns, the number of collisions will be reduced to 6 and the velocity will increase to between 0.6 m/s and 0.8 m/s. Through repeated experiments, it was found that a particle diameter range between 53 and 75 μ m is the most desirable material to be coated when a given gas flow rate is applied. Meanwhile, it was found that the powder focal length decreased from 7.43 mm to 4.46 mm when the recovery coefficient increased from 0.91 to 0.99, which provided a reference standard for screening the diameter of coaxial laser melting powder.

The pre-set powder method is simple and flexible, but the lack of inert gas protection of the powder leads to serious burnout, and the surface of the molten layer is rough and the organization is not uniform. The synchronous powder feeding method has the characteristics of high automation, fast melting speed, good molding, and material stability, which are widely used in laser melting. Among them, coaxial powder feeding powder flow is isotropic, which simplifies the problem of attitude adjustment of the laser beam and powder flow and is more applied on flat or circumferential specimens; the off-axis powder feeding structure is relatively simple and has a wide

range of applications, which is suitable for processing of complex curved parts. Compared with powder coating, the material utilization rate of the wire feeding system can reach 100%, but it has the problems of the large heat-affected zone, difficult adjustment of process parameters, and small application range.

The laser cladding nozzle is the core component of the laser cladding system, which enables the transmission, transformation, focusing, and simultaneous delivery of the laser beam and the cladding material. The coaxially delivered powder nozzle can perform the melting process in any direction and also has an indirect effect on the width of the melted layer, the spot diameter, and the melting efficiency. In recent years, some scholars have conducted theoretical and practical studies related to this field, proposing the development of new nozzles to improve the powder collection rate and the optimization of existing nozzles to reduce the powder stream dispersion while maintaining the powder usage efficiency.

The nozzle gap width and convergence angle of the YC52 Precitec laser head were analyzed for experiments by Doubenskaia M et al.[6] The nozzle gap widths were divided into two categories, which are "short" (maximum gap widths of 0.5 mm and 1.0 mm) and "medium" (maximum gap width of 1.0 mm). Through the study, it was found that the powder convergence angle depends on the nozzle tilt angle. As the gap width increased, the maximum convergence angle of both can be increased by about 10%, and the "short" nozzle with a high gap has a higher peak density and higher convergence angle, which is suitable for industrial cladding. The "medium" nozzle was suitable for dense or more concentrated powder injection. Figure 3 shows the nozzle shape geometry.

Dias Da Silva, M. et al.[7] evaluated the coaxial and off-axis nozzle process configurations in terms of three process parameters: axial motion velocity, mass flow, and power, respectively. The evaluation was based on dilution rate, water collection efficiency characteristics (proportion of material effectively adhered), and hardness as melt layer quality. It was found that the coaxial configuration showed better water collection efficiency, but higher dilution rate and lower hardness, while the off-axis configuration showed lower water collection efficiency, good dilution rate, and higher hardness. A reference standard for nozzle selection was provided in this study.

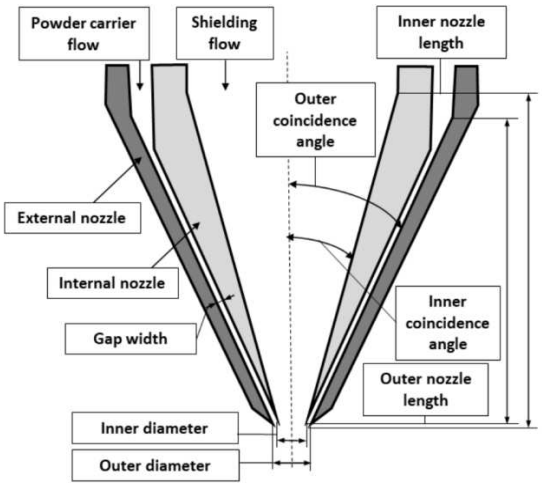

Fig. 3 *Geometry of Precitec coaxial laser cladding nozzle*

Nagulin K Y et al.[8] studied the gas powder flow using optical diagnostics to analyze and optimize the operating modes of off-axis (lateral), four-stream, and coaxial nozzles for the YC52 laser melting head, and Figure 4 shows the three nozzle designs and layouts. By modifying the design of various laser melting nozzles and optimizing the outlet diameter of the removable cyclone cap, the carrier gas flow rate was shielded and limited to improve the powder usage efficiency.

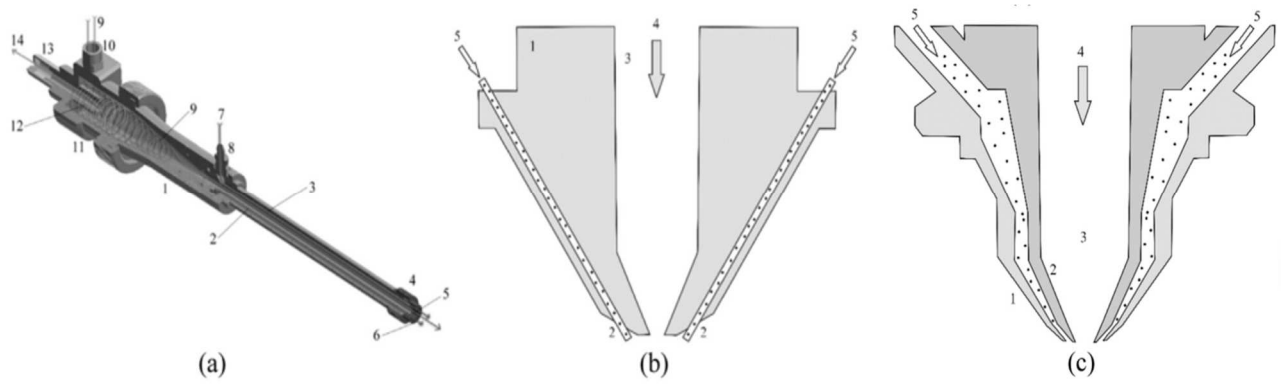

Fig. 4 *Design and distribution of the off-axis (a), four-stream (b), and coaxial (c) nozzles for the YC52 cladding head*

Leyens C et al.[9] developed a head for integrated modules based on hybrid processing that is compatible with diode, fiber, and disk lasers, locally sensing heat, and compensating for heat loss to provide sufficient energy to melt the powder. Tests had found that the device can increase the melting rate by a factor of 2-2.5, and the specially designed coaxial nozzle could handle powder volumes going up to

18 kg/hour. In total, the application of mixing technology improved the overall cladding rate and energy efficiency.

At present there are many studies related to the development and optimization of the melting nozzle, but there are still some problems, such as the structure of the nozzle needs to be optimized to reduce the loss of laser beam energy and powder to obtain a higher melting rate; the focus of the powder needs to be more accurate, especially for some high-precision two-dimensional melting or three-dimensional processing. In addition, a lot of theoretical research and experiments are needed to design nozzles adapted to different service environments and explore the nozzle support distance, nozzle exit angle, and angular position of nozzle and substrate.

3 Influence of different process parameters on the morphology of the cladding layer

The quality of the cladding layer depends mainly on process parameters such as laser power, scanning speed, powder feed, spot diameter, out-of-focus volume, and lap rate.[10] These parameters are important factors in eliminating pores and cracks, improving surface roughness, and obtaining good densities and dilution rates. The cross-influence between these parameters is also a very complex process and reasonable methods must be used to keep these parameters within the permissible limits of the laser cladding process.

3.1 Laser power

The size of the laser power determines the laser beam power density, as the laser power increases, the power density will also increase, and high power density laser input will cause rapid local heating, and when the heating rate is greater than the energy diffusion rate will lead to local temperature rise. When the temperature gradient increases, it is easy to produce residual stress inside the cladding layer after cooling, high residual stress that will lead to part deformation or cracking, and then affect the mechanical properties of the formed parts.

Koehler H. et al.[11] studied the laser melting of flat and round specimens and crank journals made of 42CrMo in turn. A fast control loop system was constructed to monitor the specimen temperature and melt pool size during the melting stage, and the power was regulated at all times. The data showed that the power at the start and end of the weld for the flat specimen was significantly higher compared to the intermediate weld section; the laser power was about 3500 W for the first rotation of the circular specimen and drops to about 2000 W after 35 seconds until the process was completed; the crankshaft weld power changed on a similar course as the circular specimen but was about 750 W higher. These result indicated that higher initial power is required for shaft parts when laser cladding is performed.

Fu F et al.[12] fused Ni60 powder on the surface of 40Cr substrate for shaft material to investigate the crack formation during the fusion process. It was found that the crack rate decreased gradually with increasing laser power, the crack depth became deeper and the crack width became thinner with other parameters remaining unchanged.

Hofman J T et al.[13] found from the experiment that at low power of 2000 W, the melt pool width increases rapidly with power and is close to the length, which appears as a visible dot on a macroscopic scale. At higher power above 3000 W, the width increases only slightly after reaching the laser spot diameter, while the melt pool length is stretched to 1.5 times the width. The magnitude of the power has a direct effect on the melt pool, and since the temperature and shape of the melt pool are relatively easy to measure, the change in melt pool shape can be used as a measure to determine the optimal power parameters.

Zhang Lei et al.[14] prepared NiCrBSi cladding layers on the surface of 45 steel piston rods, which is a common material for shafts, and investigated the effects of different powers (3.2 kW, 3.6 kW, and 4.0 kW) on the hardness and physical phase of the clad layers. At a low power of 3.2 kW, the average microhardness of the clad layer was about 2.5 times that of the base material. When the power was increased to 4.0 kW, the carbides and borides with secondary reinforcement such as CrB, Ni3B, and NiC gradually disappeared, leading to a decrease in hardness and an increase in the thickness of the clad layer.

In conclusion, insufficient laser power leads to limited melting of alloy additions, uneven surface of the clad layer, and low performance. An increase in power results in more powder being captured into the melt pool, good metallurgical bonding with the substrate, and a gradual improvement in all aspects of the clad layer properties. With a further increase in power, additional heat is used to heat the melt pool, and the temperature gradient increases. In a short time, the heat will not be transferred to other parts of the substrate, and most of the heat energy is concentrated on the surface of the molten area, forming thermal stresses, which will form cracks when the thermal stresses exceed the yield limit. At the same time, too much laser power, in the case of insufficient powder replenishment will make the substrate continue to melt, increasing the dilution rate, but also make the borides or carbides with secondary strengthening effect play deoxidation slagging ability and disappear, the hardness decreases. Therefore, choosing the appropriate power parameters can help to obtain a flat, hard, and defect-free cladding layer.

3.2 Scanning speed

The scanning speed has a great influence on the quality of the cladding layer, just like the impact of the laser power. When the speed is excessively high, the alloy powder does not melt completely, much less achieve high quality cladding. With a low speed, the melt pool is present for too long. This will make the powder to be over burned and lead to the destruction of the metal elements, which is extremely detrimental to obtaining a high performance clad layer.

Zhao Y et al.[15] studied the effects of laser cladding process parameters on the cladding width, height, and area using multiple single-factor experiments. It was found that the width of the clad layer was mainly influenced by the laser power, and the cross-sectional area, width, height, and heat-affected zone width of the clad layer increased with increasing laser power. The height of the clad layer was mainly affected by the scanning speed, the multi-track cross-sectional area and height decreased and the heat-affected zone width increased as the scanning speed increased.

Lian G et al.[16] performed a full-factor experiment by varying three factors, namely laser power, defocusing amount, and scanning speed, for the melting of W6Mo5Cr4V2 alloy powder on the crankshaft of AISI/SAE cylindrical steel. It was found that as the scanning speed increased, the width and height of the clad layer decreased and the aspect ratio decreased, and the indirect contact angle between the coating and the substrate gradually increased. When the scanning speed was 7 mm/s to 8 mm/s, the crankshaft surface was flat and the contact angle decreased at higher laser power (1800 W).

Han Yuyong et al.[17] investigated the effect of three scanning speeds of 300 mm/min, 340 mm/min, and 380 mm/min on the properties of the clad layer by melting FeCr alloy powder on the surface of 45 steel spindles. The results showed that there were no cracks and bubbles inside the clad layer at 300 mm/min and 340 mm/min, and the grains of the clad layer gradually became smaller and the microhardness increased as the scanning speed increased, and the hardness decreased after reaching 380 mm/min, and there were tiny bubbles at the bond between the clad layer and the substrate. It is concluded that the scan speed of 340 mm/min is the best scan speed to obtain the relatively high hardness of the clad layer.

Jiao X et al.[18] investigated the microstructure and properties of the clad layer by melting T15M HSS alloy powder on the surface of the Q235 substrate at three scanning speeds. The clad layer consisted of martensite, residual austenite, and carbide, with the increase of scanning speed, more carbide precipitated at the austenite grain boundaries and the local deviations decreased. The hardness of the clad layer was lowest at a scanning speed of 100 mm/min, and the abrasiveness was highest at 300 mm/min with a large amount of debris flaking. At 200 mm/min, the clad layer was finer grained and had the highest average hardness with higher solid solubility.

In summary, when the scanning speed is low, the heat input to the base material is high, which increases the deformation of the shaft parts and affects the circular runout, thus leading to failure or shortening the life of the parts. As the scanning speed increases, the heat input per unit area at the same time decreases, the solidification rate of the melt pool accelerates, the nucleation rate increases, and the number of grains increases, so the organization of the clad layer is denser and the hardness increases. However, the width and height of the clad layer are reduced due to the lower powder melting rate. Too fast scanning speed can also make the microstructure of the clad layer uneven due to insufficient energy absorption by the powder, which increases the rate of bubble defects in the bonding area.

3.3 Overlap rate and powder feed rate

The overlap rate describes the overlap of the adjacent fusion channels during the cladding process and is a key factor in the surface flatness of the machined part, while the powder feed rate determines the cladding height. These two parameters are important for the morphology of the clad layer after processing.

An Xianglong et al.[19] used Ansys software to establish a multi-pass cladding model to explore the effect of different lap rates (30%, 40%, 50%, 60%, 70%) on the residual stresses. The results show that the hardness of the clad layer increases with the increase of the lap rate, the friction coefficient first increased and then decreased, while the average and minimum values of the equivalent residual stress gradually decreased. The melt layer with a 50% lap rate was selected to obtain a good anti-wear effect with the substrate and was most suitable for subsequent processing.

The performance of the CoCrW clad layer prepared on the surface of 304 stainless steel at different lap rates was investigated by Fang Zhenxing et al.[20] The appearance of the clad layer was well formed and flat without obvious defects at a 30% lap rate, saving material while facilitating post-processing compared to 50% and 60% lap rates, and the overall microhardness reached about 450 HV, which is 2.1 times higher than the substrate and slightly higher than 40%. The essence of the lapping rate was to keep the recessed area between the melt channels in line with the lap area while minimizing the effect of local self-tempering on the cladding hardness due to the non-lap area after heating.

Jun W et al.[21] investigated the effect of Ni60AA alloy powder on 45 steel shaft surface cladding at

different laser power, powder feeding rate, and shaft speed using the polarization method. It was concluded that the powder feeding rate had the greatest influence on the thickness of the clad layer, the dilution rate (8%-15%), and the hardness (not less than 900 HV), with the increase of the powder feeding rate, the after-degree of the clad layer increased and the surface flatness decreased. Meanwhile, the higher the feeding rate, the greater the energy decay, the gradual decrease in dilution rate, and the increase in hardness.

3.4 Selection of integrated process parameters

Laser cladding is a representative multivariate and nonlinear process. Beside the influence of several single factors on the aspect ratio and dilution rate of the clad layer, it is necessary to consider the interactions between these factors. For the selection of multiple process parameters, several single-factor tests and multi-factor orthogonal tests are generally used to select the optimum combination, followed by specific comparative experiments to determine the final process parameters.

Linsen SHU et al.[22] conducted laser cladding experiments using a combination of single-factor experiments and multi-factor orthogonal tests for searching the optimal process parameters for the surface cladding of 304L alloy powder on 45 steel. The effects of several process parameters on the cladding layer height, width, and properties were investigated using extreme difference analysis, and the optimal combination of the cladding parameters was calculated by a fuzzy comprehensive evaluation.

Shu D et al.[23] melted nickel-based alloy powder on nickel-based alloy wrought plates to investigate the combined effects of parameters such as laser power, scan speed, powder feeding speed, and gas feeding speed on the melt pool width-to-height ratio and dilution rate. The research process used orthogonal experiments and a comprehensive scoring method to transform multiple indicators into a single indicator. Finally, the optimal parameters were obtained by analyzing the binary table.

Shi Y et al.[24] made a graded composite coating, specifically on 20CrMnTi alloy steel by means of laser melting.The melting test is mainly performed by the orthogonal method, and the main influencing factors are laser power, scanning speed and material flow rate of the powder. The optimum process parameters were obtained by the combined analysis of Taguchi and TOPSIS methods, and the microhardness of the melted layer was increased to three times of the substrate.

Chen Y et al.[25] studied the effect of JG-3 iron-based powder on the cladding quality of 45 steel substrate surface by using the interactive orthogonal experimental method, and the specific variables selected were laser power, scanning speed, and powder feeding speed. And the optimal process parameters were used for the experiments, the microstructure of the molten layer was finer and the performance was significantly improved, which ensured the reliability of the optimized results.

A combination of laser device characteristics and finite element simulation methods for the melting zone was used by Shi B et al.[26] The width and height of the cladding trajectory were modeled to investigate the effect of process parameters on cracking by using line energy and powder feeding rate as variables for Ni60A cladding on 45 steel surfaces. The degree of cracking of the cladding is also influenced by the line energy and the powder feeding speed. The crack distribution in the fractured part also changes from a complex lattice shape to a parallel shape as the crack disappears. The no-cracking parameter ratios were obtained experimentally.

Zheng Hui et al.[27] explored the effect of the cladding center angle α on the bending amount after machining a cladding groove on a 45-steel long shaft and clad with nickel-based 202 powder to repair the damaged area, as shown in Figure 5. α is the cladding center angle. It was found that when the cladding center angle is less than 90°, the cladding layer area and the maximum shaft bending are proportional, and conversely when the center angle is greater than 90°, the shaft bending does not change significantly. The number of cladding layers was directly proportional to the amount of shaft bending for a certain cladding area. Therefore, when repairing damaged parts of shaft parts, the center angle of the cladding should be controlled to reduce the deformation of the parts.

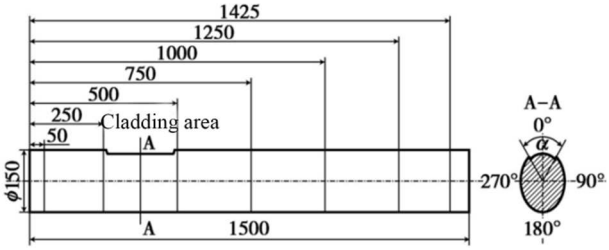

Fig. 5 *Schematic diagram of the test shaft*

4 Types of cladding materials and applications

The selection of the cladding material is an important prerequisite for obtaining a good cladding layer. In the experiments, metal powder, ceramic powder, and composite powder are often used as cladding material. Among them, self-fusing metal powders such as Fe-based, Co-based, and Ni-based are widely used and studied, such as Fe55, Fe60, Co50, Ni60, etc. Ceramic alloys include carbides (WC), borides (TiB2) and oxides (Al2O3), etc. Composite powders include oxides, nitride composite alloys, and silicide powders, etc. The materials used in the

experiments depend on their compatibility with the base material in terms of coefficient of thermal expansion and melting point, as well as the physicochemical properties after bonding.

4.1 Selection of metal-based cladding materials

Metal-based alloys are generally composed of two or more alloys, partially or fully alloyed to form a metal that can be widely used in the cladding of substrates including all types of carbon steel, alloy steel, stainless steel, and cast iron.

He Jianqun, et al.[28] melt coated Fe55 self-fusing iron-based alloy powder on the surface of 12CrNi3A steel for the shaft. After the experiment, the molten cladding layer was well bonded with the substrate, the organization was needle-like martensite, carbide particles, and a small amount of residual austenite, the average hardness reached 650 HV higher than the average hardness of the base material 276HV, and the depth of the hardened layer could reach 1.1 mm to 1.5 mm.

Xu M et al.[29] fused iron-based and nickel-based powders on the surface of 45 steel, respectively. In their experiments, they found that the bond strength of Fe-based powder was about 2.5 times greater than that of Ni-based, and the shear stress of Ni-based powder was less than half of that of Fe-based powder, which indicated that the powder type had a significant effect on the bond strength of the clad layer.

Aditya Y N, et al.[30] melt coated AerMet-100 ultra-high alloy steel powder on the surface of AISI 4340 steel, a commonly used material for shaft parts. The microstructure was slatted martensite with residual austenite. After heat treatment, the residual austenite was reduced to form fine carbides and the tensile stress was increased by a factor of 1.41.

Han T et al.[31] used a mixture of Ni, Ti, and Cr powders as raw materials to fuse clad on the surface of Q235 carbon steel specimens, a common material for shafts. It was found that the hardness of the molten layer with a Cr content of 15% could reach 1083.7 HV0.2, and its hardness and wear resistance were better than those of the molten layer with a Cr content of 30% and 45%. It was shown that too much Cr content is detrimental to improving the hardness and wear resistance of the coating.

Wang K et al.[32]verified the phase fusion on the surface of 45 steel substrates with stainless steel powders with different Mo contents using several schemes. It was found that with the increase of Mo content, the number of martensites decreased the number of ferrites gradually increased, the microhardness of the clad layer decreased the wear resistance increased. However, the wear resistance of the clad layer at 6.0% Mo wt. was about 3.7 times higher than that of the Mo-free clad layer. With the increase of Mo content, the degree of corrosion resistance of the molten cladding layer does not change linearly, its change law is first to increase and then decrease when the content is 2.0wt%, its corrosion resistance is the best. It is proven that the proper addition of some Mo can improve the material properties as well as the lifetime of the melt-clad layer.

4.2 Application of ceramic cladding materials

Ceramic materials are widely used in the shaft laser cladding process because of their high strength, high hardness, high temperature resistance and corrosion resistance. Al2O3, TiO2,TiB2 and other oxide ceramic materials containing Al or Ti, due to the larger atomic radius of Al, Ti, added to the alloy can intensify the lattice distortion obviously enhance the solid solution strengthening effect, enhance the hardness and toughness of the alloy, in addition Ti can also increase the low temperature toughness and corrosion resistance of the coating[33]. SiC, WC, TiC and other carbide ceramic materials can play a role in enhancing the phase, refining the grain size and improve wear resistance, while the introduction of Si elements is conducive to enhancing the fluidity of the melt pool and the de-oxygenation and slagging ability of the clad layer[34].

Chen L et al.[35] prepared NBC in situ enhanced iron-based coatings by fusion coating NbC with B4C powder on the surface of medium carbon steel. The coating mainly consisted of reinforcing phases (NbC, Fe2B, B4C) and substrate ([Fe-Cr] solid solution). The grain structure of the composite coating under the microscope was columnar, and the hardness of the dispersed NbC particles formed in situ at the crystal junction reached 866.36 HV0.5. It was roughly 3.95 times harder than the collective and 4.16 times harder than the iron-based coating. Comparing the average friction coefficient, the composite coating was about 0.405, which was 0.775 times that of the iron-based coating and 0.879 times that of the substrate. For the test loss, it was straight up to 1/4 of the loss of the iron-based molten coating.

Wu Q et al.[36] successfully synthesized VC-Cr7C3 ceramic composite fusion clad layer on a mild steel surface, which bonded well with the substrate. The experiments showed that the average hardness of the clad layer increased by 7 times compared with the substrate, the wear resistance increased by 4 times, and the friction coefficient fluctuation was lower, which significantly improved the physical and chemical properties of the substrate surface.

Jianing L et al.[37] prepared Al+TiC laser melting layer on the surface of Ti-6Al-4V alloy by the CO2 laser melting technique. It was found that the surface of the molten layer was free of porosity or crack defects during the increase of the mass percentage of TiC from 30% to 40%, the hardness decreased after increasing from 450 HV to 1200 HV, and the hardness

was about 650 HV and minor cracks were produced when the mass percentage reached 50%.

Studies have found that a wide range of ceramic materials can improve the performance of the clad layer significantly, but because they are not specifically created for laser cladding processes, they lack specificity in terms of laser beam energy absorption and clad layer bond strength, and require research and development of specialized materials. There are significant differences between ceramics and metals in terms of melting point and coefficient of thermal expansion, and the control of the minimum dilution rate when melting ceramic powders onto metal substrates is not as good as that of metal alloy powders. It will be found that the clad layer is prone to porosity, cracks and surface inequality. Therefore, in practical applications, metal alloy powders are still used as the mainstream cladding material and ceramic powders are mostly in the research stage.

4.3 Development of metal-ceramic composite cladding materials

The ceramic cladding material itself is brittle and difficult to process, which is limited in application. To better apply the high-quality performance of ceramic materials in practice, metal-ceramic composite materials made by powder metallurgy methods came into being. It was found that with the addition of ceramic materials, the defects such as cracks and bubbles that often appear in the original metal clad layer were eliminated, and the metal-ceramic composite clad layer had the advantages of excellent metallurgical bonding ability of metal coating and high hardness, friction resistance and corrosion resistance of the ceramic coating.

TONG W et al[38]. chose the shaft material of ductile iron as the object of study and performed a 30% TiC-Cobalt-based alloy fusion coating on its metal surface. It was found that the heat-affected zone at the junction part of the overlay layer and the substrate was mainly lamellar martensite, a small amount of residual austenite and graphite spheroid, which exhibited in addition to good metallurgical bonding phenomena. The hardness measurement shows that the maximum hardness in the overlay layer can reach 1278.8 HV0.2, while the ductile iron matrix hardness is less than one-fifth of it.

Chen L et al.[39] fused TiC with TiN enhanced nickel-based fusion coating layer on the surface of a spline shaft made of 40Cr. It was found that with the addition of TiC, the cracks and holes on the surface of the nickel-based fusion clad layer disappeared, the cermet particles were uniformly distributed, and the average hardness increased by 1.72 times, and the wear rate was 0.307 times that of the substrate. It was also discovered that the distribution of particles in ceramics is closely related to the thermal conductivity, with the lower temperature distribution being approximately uniform. It is also able to reduce the heat affected zone to transform crystals to equiaxed crystals.

Shu D et al.[40] melt-coated nano-WC-reinforced nickel-based melt-coated layers with rare earth CeO2 (0%, 0.5%, 1.0%, 1.5%, and 2.0% mass fraction, respectively) on the surface of 42CrMo steel for shafts. They found that the modified composite coatings containing CeO2 eliminated cracks to flatten the surface and significantly improved hardness and surface wear resistance. The maximum microhardness was about 1560 HV0.2 when 1% CeO2 content was added, producing a uniform diffuse strengthening effect.

Leunda J et al.[41] prepared hard WC particles reinforced NiCr-based fusion cladding layer on the surface of C60 steel, a material used for shafts. The experiments were carried out by controlling the shape and size of the WC particles and preparing defect-free fusion cladding layers of maximum thickness from three types of WC particles selected spherical fine particles, spherical coarse particles, and crushed coarse particles. From the results, it was found that spherical coarse particles and spherical fine particles obtained similar coatings, with coarse particles generating coatings showing a more uniform carbide distribution and fine particles having higher wear resistance but poorer mobility with larger porosity. Both crushed particles and spherical coarse particles melt coating layer at the same size do not have porosity, but the thickness of the former is significantly higher.

Lei J et al.[42] found that carbon fiber-reinforced nickel-based fusion clad layers have higher hardness as well as better wear properties than nickel alloy fusion clad layers, with an average increase in hardness of about 1.3 times and a reduction in wear rate to 55%.

Shi C et al.[43-44] used laser melting to prepare carbon fiber (CF) reinforced Ni-based composite fusion cladding layers (CFs/Ni) on the surface of Q235 steel. It was found that the same content of CF showed different morphology and distribution in the coating.As the CF content increases from none to 9vol%, the carbon fiber changes by increasing and then decreasing. The best organization and uniformity of distribution was achieved when the CF content is 6 vol%. The average microhardness of the molten layer of the reinforced composite was able to reach 1.7 times that of the nickel-based molten layer, while the ultimate tensile strength was 3.7 times that of the nickel-based molten layer.

In conclusion, shaft parts have to meet various performance requirements such as wear resistance, pressure resistance, corrosion resistance, and high-temperature resistance at the same time in service, and a single type of clad material is not easy to achieve the required mechanical properties in terms of hardness

and wear resistance. Composite cladding materials, as a combination of metal and ceramic materials, can be adjusted by adjusting the composition of alloying elements in ceramic and metal powders to obtain a high hard phase volume fraction and thus improve their hardness. Meanwhile, the addition of coarse ceramic particles with low thermal conductivity in the composite can promote the crystal shift from columnar to the equiaxed body, further reduce the range of heat-affected zone and improve the stability of the clad layer, which is a research direction for future clad materials.

5 Application of numerical simulation techniques in laser cladding of shaft components

The traditional research process of laser cladding of shafts requires controlling each factor in turn and conducting several experiments to find the ideal parameters, which consumes a lot of material and energy. Among them, parameters such as melt pool shape, substrate, and surface stress of the clad layer change rapidly with laser movement and are cost-effective to measure using existing equipment. Numerical simulation techniques can effectively and accurately study the distribution of temperature and stress fields that are difficult to capture during laser cladding and the planning and prediction of trajectories. Then, defects such as cracks and porosity can be reduced by improving the process flow, optimizing process parameters, or improving the melting powder. Numerical simulation techniques are complementary to experiments and are of great importance in the process of laser cladding of shafts.

5.1 Numerical simulation of temperature fields in laser cladding

Laser cladding processes are often accompanied by large heat changes and complex heat and mass transfer phenomena. Moreover, the high cooling rate due to the local heat input from the laser beam promotes significant microstructural changes in the heat-affected zone, leading to metallurgical defects associated with sub-stable phases in the melting layer and heat-affected zone. Accurate and reliable simulation of the temperature field in various parts of the laser cladding process can help to understand the temperature distribution during the cladding process and select a suitable and effective method to improve the quality of the clad layer and increase the service life of the shaft components.

Guo S et al.[45-46] applied single-pass multilayer laser cladding to a rotor shaft using the raw and dead cell method in ANSYS. A section of the rotor shaft was selected experimentally for temperature result analysis, and the temperature distribution curve and temperature cloud plot with time were obtained. Subsequently, Fe60 powder was melted on the 45 steel rotor shaft, and the measured results were in general agreement with the simulation results with an error of less than 10%.

Li C et al.[47] developed a multi-field coupled three-dimensional mathematical model of Fe60 powder melting on a 45 steel substrate to calculate the transient change profiles of temperature at different locations during laser melting. Considering the possible influences in the experiment, such as convection and diffusion of the movable melt pool, this is used to predict the morphology and structure of the melt pool during solidification. The same parameters were taken for experimental verification and the simulation results agree well with the experimental data confirming the simulation accuracy.

Cui L J et al.[48] used mainly conducted simulations as a means to study the dynamic changes in the temperature field of shaft materials. ANSYS finite element analysis software was used to simulate the melting of 316L alloy powder on the surface of 45 steel. During the study, the continuous discrete method and raw and dead cells were introduced for calculation, and the temperature field variation distribution maps of each node of different paths at different times and locations as well as the amplitude of temperature field distribution of each node were generated to determine the temperature distribution of the substrate surface cooling process. It was also found that with the increase of cooling time, the amplitude of temperature decrease decreases in a nonlinear manner, and the temperature field distribution at different locations tends to be constant. The experimental comparison error results were less than 10%.

The numerical simulation of the temperature field of laser cladding is beneficial to deducing the evolution of the organization and structure of the cladding layer, but there are still some problems to be solved at this stage. For example, the simulation only shows the macroscopic process and results of temperature change, the internal temperature of the melt pool cannot be observed, and the related parameters such as thermal properties of various materials involved are not perfect, as well as the weakness of the auxiliary software on the influencing factors such as powder utilization rate, oxygen content, metal vaporization, and convective heat transfer coefficient can also lead to errors with the actual results. In addition, more boundary conditions, such as convection, buoyancy, radiation, latent heat, and other factors should be considered in the research process, and the microstructure and thermodynamics should be combined in the numerical simulation to make the simulation results closer to the actual.

5.2 Numerical simulation of stress fields in laser cladding

When laser cladding is processed, the high-temperature part of the substrate is thermally expanded and the rapid flow of material is constrained by the low-temperature region of the material, resulting in more complex thermal stresses and plastic deformation and cracking. After the shaft part is cooled to room temperature, the tendency of the material to return to its original state leads to residual stresses in the cladding layer, and high residual stresses also lead to plastic deformation and cracking of the shaft. The numerical simulation of the stress field allows us to understand the distribution of stresses during the laser cladding process and to prevent and eliminate cracks, holes, and impurities promptly.

Shu Linsen et al.[49-50] established a mathematical model for the nonlinear transient analysis of the wear axis surface laser cladding test to obtain the three-dimensional temperature and thermal stress distribution law during the cladding process. The results showed that the nodal stress distribution pattern was consistent with the transient melting temperature gradient, and the stresses after cooling were concentrated in the heat-affected zone and close to the edge side of the cladding material. The simulation results are in high agreement with the experimental results, and the error of the residual stress results can be guaranteed to be within 10%, thus proving that the simulation can predict the residual stresses in the parts.

Hutasoit N et al.[51] used numerical simulations to investigate the stress changes in cobalt-based and nickel-based alloys when they were fused to the surface of AISI 4130 substrates, respectively. It was found that higher compressive residual stresses existed in the cobalt-based alloy specimen substrate and lower tensile residual stresses existed in the fused cladding layer compared to the nickel-based. It was also shown that the thickness of the cladding layer is inversely proportional to the fatigue life for the same structural dimensions of the part. The simulation results were verified experimentally with a maximum error of about 7%.

Cui Z et al.[52] performed laser cladding on a 12CrNi2 alloy steel diesel engine shaft and established a three-dimensional finite element model using ABAQUS software and DFLUX heat source subroutine. And they analyzed the variation of thermal and residual stresses present on the shaft surface when the temperature changes the thermophysical parameters and the conditions of the influence of the latent heat of phase change on the temperature field. Moreover, the pattern of residual stresses in the heat-affected zone between the clad layers and the cooling time was also investigated.

Nazemi N et al.[53-54] used a three-dimensional thermodynamic finite element model to simulate the residual stresses generated during the fusion cladding of P420 stainless steel powder on an AISI 1080 substrate. The model predicts the residual stresses in the transverse and longitudinal directions at the surface of the molten clad layer, at the intersection, and in the substrate. Through the model, it was concluded that the longitudinal and transverse stresses in the interfacial region are essentially tensile stresses, which agreed with the experimental results measured by the X-ray diffraction technique.

Shao Y P et al.[55] developed a three-dimensional model of the temperature and residual stress fields for simulated analysis of the melting of iron-based alloys on the surface of 304 steel using a rectangular laser beam. During laser beam exposure, the stress change in the clad layer was tensile-compressive-tensile, the longitudinal residual stresses far exceeded the transverse residual stresses, and the maximum transverse residual tensile stress was generated at the junction of the clad layer and the substrate, and the longitudinal residual tensile force in the clad layer was larger than that in the substrate.

Stress changes during laser cladding are complex, and current models provide rough estimates of stress changes that need to be improved in terms of accuracy. Scholars can start with the heat source to explore the most suitable heat source model for the working conditions, and can also consider the effects of substrate and cladding layer dimensions, internal stresses in the cladding material, and the coefficient of thermal expansion when modeling, but it also brings a lot of computational and experimental work.

5.3 Trajectory planning for laser cladding

For some common shaft parts, the best scanning path for the laser beam is to spiral along the part surface. This process consists of two motions, one is the rotation motion of the shaft part around the centerline and the other is the interpolation motion of the laser beam along the part bus, as in Figure 6. A certain coupling between these two motions has to be achieved in order to obtain a good cladding layer.

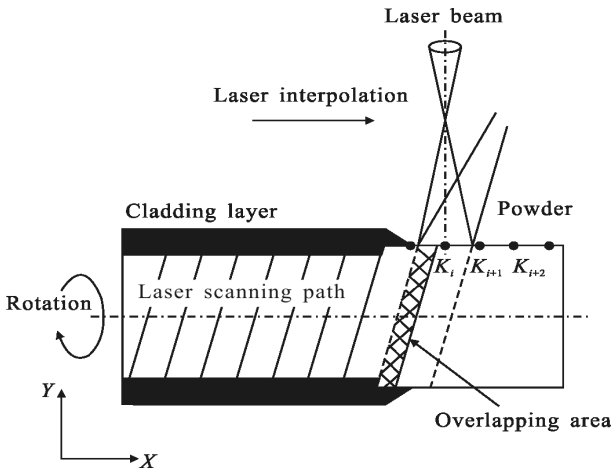

Fig. 6 *Principle diagram of shaft components laser cladding*

For the laser cladding remanufacturing of complex shaft parts, it is difficult to achieve trajectory planning and automatic programming. To address this situation, Huang, Yong et al.[56] proposed a NURBS curve isometric interpolation method for planning the laser beam attitude and scanning path of the lateral powder feed nozzle by combining reverse engineering and shaft remanufacturing characteristics as shown in Figure 7. The experiments were carried out by the method of linear interpolation of the electron microscope scale to measure the thickness of the molten cladding layer at four locations, as shown in Figure 8. It was found that the metallurgical bonding of the molten cladding layer with the substrate was good, and the hardness was significantly increased, and the laser beam centerline at 1-1 reached the experimental maximum angle of 42 ° with the horizontal. Due to the effect of gravity on the powder, the light-powder fit was poor, and the thickness of the molten layer was minimal, but only 0.034 mm less than the maximum thickness at 1-3, and the thickness difference was within a reasonable range.

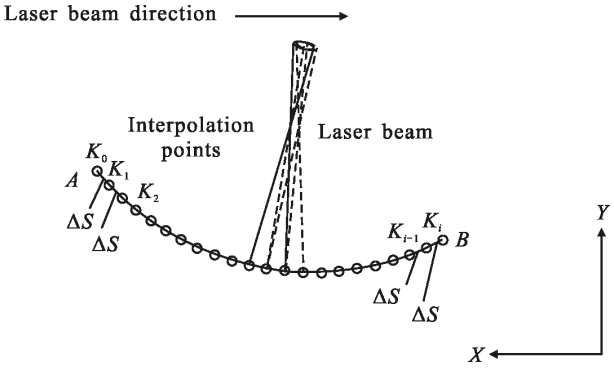

Fig. 7 *Constant arc increment interpolation method*

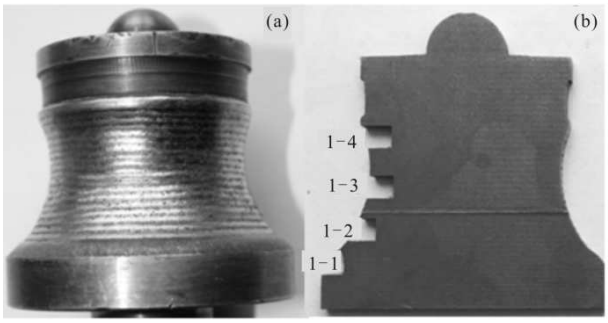

Fig. 8 *Location map of the cladding layer specimen*

Feng Hui et al.[57] fused a Fe-based alloy powder on the surface of a crankshaft connecting rod journal made of 45 steel. During the experiment, the connecting rod journal moved around the main journal in a circular motion and the laser beam followed the journal motion. The relationship model between the trajectory of the laser beam and the motion of the rotating journal (as in Figure 9) and the relative velocity during laser cladding of crankshaft connecting rod journals was thus derived.

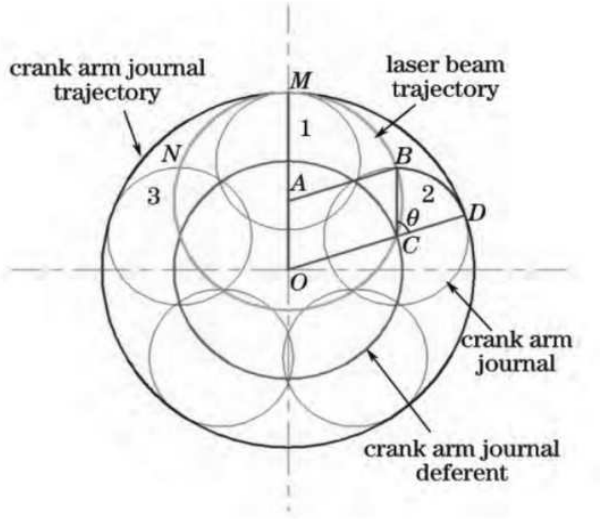

Fig. 9 *Trajectory curve for laser cladding process*

Liu L et al.[58] combined reverse engineering to reconstruct the broken region morphology, and sliced curve sets were extracted in the scanning direction for the damaged region. Within a specific step set point, they collated the laser beam axial vector information by a biasing algorithm to obtain the camshaft surface fusion trajectory model.

Wang X et al.[59] proposed a path planning method based on the characteristics of thelaser cladding process. The method was based on the path planning of the point cloud data of the surface obtained by reverse scanning (Figure 10 showed the point cloud slice simulation), and the normal vector was obtained by NURBS (non-uniform rational B-sample) surface fitting to realize the continuous variable position melting motion of the robot. This was of great importance for the laser cladding trajectory planning of camshafts.

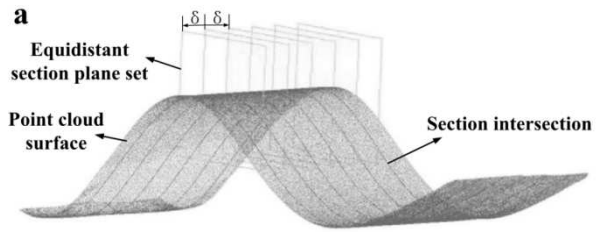

Fig. 10 *Point cloud slice simulation*

Li Y et al.[60] designed different types of grooves on the surface of ductile iron QT500-7, a common material for drive shafts, to investigate the properties of nickel-copper alloy fusion clad materials. It was concluded that the annular groove and cross fusion cladding processes are beneficial in reducing residual stresses.

Most of the surface laser cladding path planning for shaft parts is based on CAD model reconstruction

techniques, which increases the computational difficulty when complex surfaces such as crankshafts are involved. The research on surface laser cladding trajectory generation method is not mature, there is no detailed treatment point extraction scheme, and the methods of obtaining normal vectors vary, these problems can be solved to obtain higher quality cladding layer for the parts.

6 Conclusion

Shaft parts are one of the common and important parts in machinery and equipment, playing the role of supporting the rotating parts and rotating with them to transmit motion, torque or bending moment, etc.. In addition to its own fatigue fracture, it also needs to overcome the working environment in the sliding surface part of the summary of small burns and surface damage, corrosive gases and hard impurities caused by the scratch and the temperature difference between the work of the components and the thermal deformation caused by permanent bending. As the "umbrella" of the part, the cladding layer protects the substrate, reduces wear, strengthens the hardness, and thus improves its working accuracy and life. However, different cladding processes are required for different cladding conditions. Therefore, to obtain a cladding layer with good physical and chemical properties, it is important to investigate and summarize the influencing factors such as selection and development of process equipment, optimization of comprehensive parameters, and combination of cladding materials.

In the future, the aspects of closed-loop control, melt pool shape monitoring, and improving the reliability of numerical simulation should be explored. By studying a stable and efficient closed-loop control system for curved surface laser melting, the process parameters, the deflection angle of the melting head and the temperature dimensions of the melt pool can be intelligently monitored in real-time to improve the melting quality. At the same time, the melt cell, as the smallest forming unit in the process, can be optimized by keeping its shape, size, and temperature within the appropriate range, which in turn can improve the efficiency of the research, and also highlights the importance of developing the relevant hardware to ensure accurate monitoring. For numerical simulations, adding simulations of melt cell temperature field, stress field, and fluid field, and coupling thermal, mechanical, and microstructure analysis while optimizing the system moving heat source model, convective heat transfer coefficient, and considering more minor influencing factors such as metal vaporization and oxygen content can help improve the accuracy of prediction. In addition, the mechanism of bubbles and cracking on the coating surface should continue to be studied in depth to improve the preventive measures that need to be taken during the laser cladding process. Such as trying to reduce the content of B, Si, and C in the powder, to reduce its capacity to oxygenate and create slag, so the bubbles in the melt pool can not float in time, and increase the crack sensitivity; or choose a defect-free substrate and preheat, maintain the temperature at 200-400 ℃, to reduce the temperature gradient between the substrate and the cladding layer, improve the cladding layer denseness, etc. This set of tasks can greatly enhance the appearance cladding of the shaft part, thus increasing their working accuracy and extending their service life.

Acknowledgement

This work was financially supported by Science and Technology Project of Jilin Provincial Science and Technology Department of China (20200201220JC); Jilin Provincial Education Department Science and Technology Plan Project (JJKH20220589CY), and authors wish to express their gratitude.

References

[1] CHANGSAI, L., YUJIANG, W., ZHONGQI, S., SHICHENG, W., LIANG, Y., YUEBIN, L. (2018). State-of-arts and perspectives of crankshaft repair and remanufacture. In: *Materials Review*, Vol. 32, No. 1, pp. 141-148.

[2] MITTAL, K.L., BAHNERS, T, (2007). Laser Surface Modification and Adhesion, pp. 203-262. *China Machine Press*, John Wiley & SonsIn. ISBN

[3] ABIOYE, T.E., FARAYIBI, P.K., CLARE,A.T. (2017). A comparative study of Inconel 625 laser cladding by wire and powder feed stock. In: *Materials and Manufacturing Processes*, Vol. 32, No. 14, pp. 1653-1659.

[4] FARAYIBI, P.K., ABIOYE, T.E., CLARE, A.T. (2016). A parametric study on laser cladding of Ti-6Al-4Vwire and WC/W2C powder. In: *International Journal of Advanced Manufacturing Technology*, Vol. 87, No. 5, pp. 3349-3358.

[5] LIU, H., HE, X., YU, G., WANG, Z., LI, S., ZHENG, C. (2015). Numerical simulation of powder transport behavior in laser cladding with coaxial powder feeding. In: *Science China Physics*, Mechanics & Astronomy, Vol. 58, No. 10, pp. 1-10.

[6] DOUBENSKAIA, M., KULISH, A., SOVA, A., PETROVSKIY, P. (2021). Experimental and numerical study of gas-powder flux in coaxial laser cladding nozzles of Precitec. In:

Surface and Coatings Technology, Vol. 406, No. 10, pp. 126672.

[7] DA SILVA, M. D., PARTES, K., SEEFELD, T., VOLLERTSEN, F. (2012). Comparison of coaxial and off-axis nozzle configurations in one step process laser cladding on aluminum substrate(Article). In: *Journal of Materials Processing Technology*, Vol. 212, No. 11, pp. 2514-2519.

[8] NAGULIN K.Y., ISKHAKOV F.R., SHPILEV A I. (2018). Optical diagnostics and optimization of the gas-powder flow in the nozzles for laser cladding. In: *Optics & Laser Technology*, Vol. 108, No. 1, pp. 310-320.

[9] SILVELLO, A., PERRONE, A. (2021). Laser Cladding of Metals, pp. 197-247. *Springer*, Pasquale. ISBN

[10] ZHU, L., XUE, P., LAN, Q., MENG, G., REN, Y., YANG, Z. (2021). Recent research and development status of laser cladding: A review. In: *Optics & Laser Technology*, Vol. 138, No. 1, pp. 106915.

[11] KOEHLER, H., PARTES, K., SEEFELD, T. & VOLLERTSEN, F. (2010). Laser reconditioning of crankshafts: From lab to application. In: *Physics Procedia*, Vol. 5, No. 1, pp. 387-397.

[12] FU, F., ZHANG, Y., CHANG, G., & DAI, J. (2016). Analysis on the physical mechanism of laser cladding crack and its influence factors. In: *Optik*, Vol. 127, No. 1, pp. 200-202.

[13] HOFMAN, J.T., DE LANGE, D.F., PATHIRAJ, B. (2011). FEM modeling and experimental verification for dilution control in laser cladding. In: *Journal of Materials Processing Technology*, Vol. 211, No. 2, pp. 187-196.

[14] ZHANG, L., CHEN, X.,ZHANG, K., JIANG, Z., MAO, P., FU, L. (2019). Microstructure and Wear/Corrosion Resistance of Laser Cladding Ni-Based Coating on Hydraulic Piston Rod for Coastal Sluice. In: *Materials Protection*, Vol. 52, No. 11, pp. 117-22.

[15] ZHAO, Y., GUAN, C., CHEN, L. (2020). Effect of process parameters on the cladding track geometry fabricated by laser cladding. In: *Optik*, Vol. 223, No. 1, pp. 165-447.

[16] LIAN, G., ZHAO, C., ZHANG, Y. (2021). Forming control in single-track laser cladding on crankshaft based on multi-objective optimization. In: *JOM*, Vol. 73, No. 12, pp. 4319-4327.

[17] HAN, Y., LU, J., LI, J., SUN, J., LIU, Y. (2015). Lathe spindle remanufacturing based on laser cladding technology. In: *China Surface Engineering*, Vol. 28, No. 6, pp. 147-153.

[18] JIAO, X., WANG, J., WANG, C., GONG, Z., PANG, X., & XIONG, S. (2018). Effect of laser scanning speed on microstructure and wear properties of T15M cladding coating fabricated by laser cladding technology. In: *Optics and Lasers in Engineering*, Vol. 110, No. 1, pp. 163-171.

[19] AN, X.L., WANG, Y.L., JIANG, F.L., ZHANG J., ZHANG, J.Y. (2021). Effect of overlap rate on the temperature field and residual stress distribution in 42CrMo laser clad layersy. In: *Chinese Journal of Lasers*, Vol. 48, No. 10, pp. 95-106.

[20] FANG, Z.X., QI, W.J., LI, Z.Q. (2021). Effect of laser Effect of laser cladding lap ratio of 304 stainless steel on microstructure, wear resistance and corrosion resistance of CoCrW coating. In: *Materials Reports*, Vol. 35, No. 12, pp. 12123-12129.

[21] JUN. W., DONGDONG, Z., RICHU, Y. (2016). Parameters optimization and friction and wear properties for laser cladding Ni60AA coating on 45 steel shaft surface. In: *Laser & Optoelectronics Progress*, Vol. 58, No. 11, pp. 1114008.

[22] LINSEN, S., BO, W., YAYIN, H. (2019). Optimization of process parameters of laser cladding 304L alloy powder based on orthogonal experiment. In: *Mechanical Engineering Science*, Vol. 1, No. 2, pp. 10-21.

[23] SHU, D., DAI, S., SUN, J. (2020). Parameters Research on optimization of laser cladding process parameters based on orthogonal experimental method. In: *Key Engineering Materials*, Vol. 1, No. 2, pp. 10-21.

[24] SHI, Y., LI, Y., LIU, J. (2018). Investigation on the parameter optimization and performance of laser cladding a gradient composite coating by a mixed powder of Co50 and Ni/WC on 20CrMnTi low carbon alloy steel. In: *Optics & Laser Technology*, Vol. 99, No. 2, pp. 256-270.

[25] CHEN, Y., WANG, X., ZHAO, Y. (2020). Interactive optimization of process parameters and coating analysis of laser cladding JG-3 powderl. In: *The International Journal of Advanced Manufacturing Technology*, Vol. 107, No. 5, pp. 2623-2633.

[26] SHI, B., LI, T., GUO, Z. (2022). Selecting process parameters of crack-free Ni60A alloy

coating prepared by coaxial laser cladding. In: *Optics & Laser Technology*, Vol. 149, No. 5, pp. 107805.

[27] HUI,Z., ZHIREN, H., JIANG, C. (2010). Experimental investigation on shaft straightening based on laser cladding. In: *Journal of Northeastern University(Natural Science)*, Vol. 31, No. 12, pp. 1729-1732.

[28] JIANQUN, H., CHENGWU, W., JINGWEN, W., WENTAO, W., ZHIWEI, L., JINGWEI, H., ZIQIANG, Y., WEI, C. (2021). Laser cladding remanufacturing technology of 12CrNi3A steel camshaft. In: *Heat Treatment of Metals*, Vol. 46, No. 2, pp. 0254-6051.

[29] XU, M., LI, J., JIANG, J. (2015). Influence of powders and process parameters on bonding shear strength and micro hardness in laser cladding remanufacturing. In: *Procedia Cirp*, Vol. 29, No. 2, pp. 804-809.

[30] ADITYA, Y.N., SRICHANDRA, T.D., TAK, M. (2021). To study the laser cladding of ultra high strength AerMet-100 alloy powder on AISI-4340 steel for repair and refurbishment. In: *Materials Today: Proceedings*, Vol. 41, No. 1, pp. 1146-1155.

[31] HAN, T., XIAO, M., ZHANG, Y. (2019). Effect of Cr content on microstructure and properties of Ni-Ti-xCr coatings by laser cladding. In: *Optik*, Vol. 179, No. 1, pp. 1042-1048.

[32] WANG, K., CHANG, B., CHEN, J. (2017). Effect of molybdenum on the microstructures and properties of stainless steel coatings by laser cladding. In: *Applied Sciences*, Vol. 7, No. 10, pp. 1065.

[33] YA, S., CHANGJUN, W., YA, L.,HAOPING, P., (2019). Xuping, Su. Impact of alloying elements on the phase composition and mechanical properties of the CoCrFeNi-based high entropy alloys: A Review, In: *Materials Reports*, Vol. 33, No. 7, pp. 1169-1173.

[34] SHIXIN, C., WEINING, L.,WEIBIN, REN., BING, X. (2021). Microstructures and performance of laser cladding and quenching remanufactured cladding layer on QT700 ductile cast iron gear surface. In: *Laser & Optoelectronics Progress*, Vol. 58, No. 5, pp. 186-193.

[35] CHEN, L., YU, T., XU, P. (2021). In-situ NbC reinforced Fe-based coating by laser cladding: Simulation and experiment. In: *Surface and Coatings Technology*, Vol. 412, No. 3, pp. 127027..

[36] WU, Q., LI, W., ZHONG, N,. (2013). Microstructure and wear behavior of laser cladding VC − Cr7C3 ceramic coating on steel substrate. In: *Materials & design*, In: Vol. 49, No. 7, pp. 10-18.

[37] JIANING, L., CHUANZHONG, C., LEI, Z. (2011). Microstructure characteristics of Ti3Al/TiC ceramic layer deposited by laser cladding. In: *International Journal of Refractory Metals and Hard Materials*, Vol. 29, No. 1, pp. 49-53.

[38] TONG, W., ZHAO, Z., ZHANG, X. (2017). Microstructure and properties of TiC/Co-Based alloy by laser cladding on the surface of nodular graphite cast Iron. In: *Acta Metall Sin*, Vol. 53, No. 4, pp. 472-478.

[39] CHEN, L., ZHAO, Y., CHEN, X. (2021). Repair of spline shaft by laser-cladding coarse TiC reinforced Ni-based coating: Process, microstructure and properties. In: *Ceramics Internationa*, Vol. 47, No. 21, pp. 30113-30128.

[40] SHU, D., CUI, X., LI, Z. (2020). Effect of the rare earth oxide CeO2 on the microstructure and properties of the nano-WC-reinforced Ni-based composite coating. In: *Metals*, Vol. 10, No. 3, pp. 383.

[41] LEUNDA, J., SANZ, C., SORIANO, C. (2016). Laser cladding strategies for producing WC reinforced NiCr coatings inside twin barrels. In: *Surface and Coatings Technology*, Vol. 307, No. 3, pp. 720-727.

[42] LEI, J., SHI, C., ZHOU, S. (2018). Enhanced corrosion and wear resistance properties of carbon fiber reinforced Ni-based composite coating by laser cladding. In: *Surface and Coatings Technology*, Vol. 334, No. 2, pp. 274-285.

[43] SHI, C., LEI, J., ZHOU, S. (2018). Microstructure and mechanical properties of carbon fibers strengthened Ni-based coatings by laser cladding: The effect of carbon fiber contents. In: *Journal of Alloys and Compounds*, Vol. 744, No. 2, pp. 146-155.

[44] YANG, G., XIE, Y., ZHAO, S., ET al. (2022). Methods and mechanism of powder mixing for selective laser melting. In: *Manufacturing Technology*, Vol. 22, No. 1, pp. 102-110.

[45] GUO, S., YU, J., CUI, L. (2021). Numerical simulation and experimental investigation of coaxiality change of laser cladding rotor shaft. In: *Optical Engineering*, Vol. 60, No. 12, pp. 124106.

[46] MRÁZEK, M., SEDLÁČEK, F., SKOVAJSA, M. (2020). Design of composite disc spring for automotive suspension with using numerical simulation. In: *Manufacturing Technology*, Vol. 20, No. 4, pp. 525-531.

[47] LI, C., YU, Z., GAO, J. (2019). Numerical simulation and experimental study of cladding Fe60 on an ASTM 1045 substrate by laser cladding. In: *Surface and Coatings Technology*, Vol. 357, No. 2, pp. 965-977.

[48] CUI, L.J., ZHANG S.H., GUO, S. (2019). Temperature field simulation and experimental analysis of laser cladding 45 steel. In: *Optics & Laser Technology*, Vol. 57, No. 12, pp. 11-17.

[49] LINSEN, S., JIASHENG, W., HAIQING, B., YAJUAN, H. (2019). Numerical and experimental investigation on laser cladding treatment of wear shaft surface. In: *Chinese Journal of Mechanical Engineering*, Vol. 55, No. 9, pp. 217-223.

[50] KOREČEK, D., SOLFRONK, P., SOBOTKA, J. (2020). Numerical simulation as a tool to predict sheet metal forming process of TRIP Steel HCT690. In: *Manufacturing Technology*, Vol. 20, No. 5, pp. 625-631.

[51] HUTASOIT, N., LUZIN, V., BLICBLAU, A. (2015). Fatigue life of laser clad hardfacing alloys on AISI 4130 steel under rotary bending fatigue test. In: *International Journal of Fatigue*, Vol. 72, No. 1, pp. 42-52.

[52] CUI, Z., HU, X., DONG, S. (2020). Numerical simulation and experimental study on residual stress in the curved surface forming of 12CrNi2 alloy steel by laser melting deposition. In: *Materials*, Vol. 13, No. 19, pp. 4316.

[53] NAZEMI, N., URBANIC, J., ALAM, M. (2017). Hardness and residual stress modeling of powder injection laser cladding of P420 coating on AISI 1018 substrate. In: *The International Journal of Advanced Manufacturing Technology*, Vol. 93, No. 9, pp. 3485-3503.

[54] KHARROUBI, F., FERTAT, M., EL, HASSANI, S., ET AL. (2021). Simulation and control of a marine ship model's diesel engine using Python and Matlab/Simulink[J]. In: *Manufacturing Technology*, Vol. 21, No. 4, pp. 483-491.

[55] SHAO, Y.P., XU, P., TIAN, J.Y. (2021). Numerical simulation of the temperature and stress fields in Fe-Based alloy coatings produced by wide-band laser cladding. In: *Metal Science and Heat Treatment*, Vol. 63, No. 5, pp. 327-333.

[56] YONG, H., WENLEI, S., YING, C. (2017). Trajectory planning of laser cladding remanufacturing for complex shaft shaped part. In: *Infrared and Laser Engineering*, Vol. 46, No. 5, pp. 1327-133.

[57] HUI, F., JIANFENG, LI., JIE S. (2014). Numerical simulation of the temperature and stress fields in Fe-Based alloy coatings produced by wide-band laser cladding. In: *Chinese Journal of Lasers*, Vol. 41, No. 8, pp. 86-91.

[58] LIU, L., YANG, X. (2011). Path planning of laser remanufacturing robot based on reverse engineering. In: *Chinese Journal of Lasers*, Vol. 38, No. 7, pp. 0703008-4.

[59] WANG, X., SUN, W., CHEN, Y. (2018). Research on trajectory planning of complex curved surface parts by laser cladding remanufacturing. In: *The International Journal of Advanced Manufacturing Technology*, Vol. 96, No. 5, pp. 2397-2406.

[60] LI, Y., DONG, S., YAN, S. (2018). Surface remanufacturing of ductile cast iron by laser cladding Ni-Cu alloy coatings. In: *Surface and Coatings Technology*, Vol. 347, No. 1, pp. 20-28.